

# The Role of Bimetallic Thiophene-Bridged Complexes in Homogeneous Desulfurization Reactions

Michael S. Palmer and Suzanne Harris\*

Department of Chemistry, University of Wyoming, Laramie, Wyoming 82071-3838

Received December 17, 1999

A detailed study of bimetallic thiophene-bridged complexes, formed by coordination of a second metal fragment to a transition-metal-inserted thiophene complex, is reported. The bonding interactions between mononuclear metallathiacycles and a second metal center, the effects of coordination of a second metal center on the M–C and M–S bonds of the heterocycle, the stability of bimetallic thiophene-bridged complexes, and their possible role in homogeneous desulfurization reactions are addressed. Fenske–Hall molecular orbital calculations on the square-planar, transition-metal-inserted benzothiophene (BT) complex (dippe)Ni( $\eta^2$ -S,C-BT) (**6**) (dippe = (*i*-Pr<sub>2</sub>PCH<sub>2</sub>)<sub>2</sub>) and the bimetallic bridged adduct [(dippe)Ni]<sub>2</sub>( $\eta$ -BT) (**7**) show that the [(dippe)Ni] fragment coordinates to **6** via a  $\sigma$  interaction to the sulfur atom and a  $\pi$ -bonding/back-bonding interaction to the C–C double bond of the heterocycle. Both interactions are weak, and coordination of the second [(dippe)Ni] fragment has little effect on the electronic structure of **6**, suggesting that coordination, by itself, does not lead to bond activation. The thermodynamic stability of bimetallic thiophene-bridged adducts is primarily determined by the strength of the interaction between the HOMO of the coordinating metal fragment and the LUMO of the metal-inserted thiophene. Calculations indicate that this interaction is favored in complexes containing earlier, first-row transition metals and T or BT. Our calculational results, along with supporting literature reports, suggest that bimetallic thiophene-bridged complexes may lead to formation of a trimetallic  $\mu^3$ -coordinated-sulfur intermediate which could be responsible for the S–C bond activation observed in desulfurization reactions of several bimetallic thiophene-bridged complexes.

## Introduction

Thorough desulfurization of heteroaromatics such as thiophene (T), benzothiophene (BT), and dibenzothiophene (DBT) has become increasingly important as environmental regulations governing sulfur limits in high-grade fuels have become more stringent.<sup>1</sup> Although limited knowledge about key mechanistic features of hydrodesulfurization (HDS) continues to hinder progress toward more complete desulfurization, modeling complex heterogeneous HDS processes with organometallic complexes has afforded a wealth of information.<sup>2–5</sup> Work continues in a number of areas, but considerable attention has been given to the S–C bond cleavage step since desulfurization is necessarily dependent on it. One of the more interesting methods of bond activation in homogeneous systems occurs when an electron-rich transition metal inserts into one of the S–C bonds of a thiophenic molecule. This model is particularly important because certain metal-inserted complexes react further with hydrogen sources to generate hydro-

genation, hydrogenolysis, or desulfurization products in manners possibly related to heterogeneous HDS catalysis.<sup>5</sup> Despite the success of these systems, the emerging consensus is that multiple metal centers are necessary to efficiently cleave *both* S–C bonds.<sup>6–15</sup>

Some researchers have reported reactions of metal-inserted thiophene complexes with secondary metal sources.<sup>6,7,16</sup> In one of the more intriguing systems, Jones has reported that reaction of [(dippe)NiH]<sub>2</sub> with DBT results in formation of the mononuclear [Ni(dippe)]-inserted (dippe = (*i*-Pr<sub>2</sub>PCH<sub>2</sub>)<sub>2</sub>) product **1**

(1) Topsøe, T.; Clausen, B. S.; Massoth, F. E. *Hydrotreating Catalysis*; Springer-Verlag: Berlin, 1996.

(2) Angelici, R. J. *Coord. Chem. Rev.* **1990**, *105*, 61–76.

(3) Rauchfuss, T. B. In *The Coordination Chemistry of Thiophenes*; Rauchfuss, T. B., Ed.; John Wiley & Sons: New York, 1991; Vol. 39, pp 259–329.

(4) Angelici, R. J. *Polyhedron* **1997**, *16*, 3073–3088.

(5) Bianchini, C.; Meli, A. *Acc. Chem. Res.* **1998**, *31*, 109–116, and references therein.

(6) Dullaghan, C. A.; Zhang, X.; Greene, D. L.; Carpenter, G. B.; Sweigart, D. A. *Organometallics* **1998**, *17*, 3316–3322.

(7) Bianchini, C.; Jiménez, M. J.; Meli, A.; Moneti, S.; Patinec, V.; Vizza, F. *Organometallics* **1997**, *16*, 5696–5705.

(8) Ogilvy, O. E.; Draganjac, M.; Rauchfuss, T. B.; Wilson, S. R. *Organometallics* **1988**, *7*, 1171–1177.

(9) Arce, A. J.; Karam, A.; Sanctis, Y. D.; Machado, R.; Capparelli, M. V.; Manzur, J. *Inorg. Chim. Acta* **1997**, *254*, 119–130.

(10) Riaz, U.; Curnow, O.; Curtis, M. D. *J. Am. Chem. Soc.* **1991**, *113*, 1416–1417.

(11) Curtis, M. D.; Druker, S. J. *J. Am. Chem. Soc.* **1997**, *119*, 1027–1036.

(12) Jones, W. D.; Chin, R. M. *J. Am. Chem. Soc.* **1994**, *116*, 198–203.

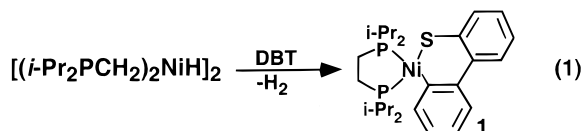
(13) Jones, W. D.; Chin, R. M.; Hoaglin, C. L. *Organometallics* **1999**, *18*, 1786–1790.

(14) Vicić, D. A.; Jones, W. D. *Organometallics* **1999**, *18*, 134–138.

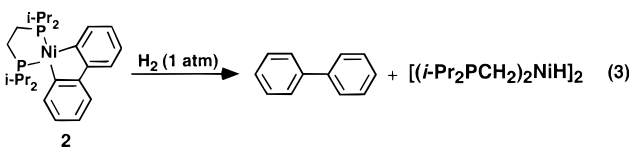
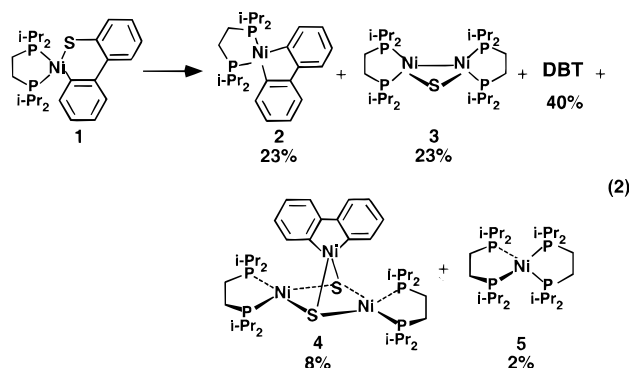
(15) Matsubara, K.; Okamura, R.; Tanaka, M.; Susuki, H. *J. Am. Chem. Soc.* **1998**, *120*, 1108–1109.

(16) Vicić, D. A.; Jones, W. D. *J. Am. Chem. Soc.* **1999**, *121*, 7606–7617.

(eq 1).<sup>16,17</sup> Complex **1** converts to four new organome-



tallic products within 5 days at room temperature (eq 2). Desulfurization can then be achieved by reaction of **2** with 1 atm of H<sub>2</sub> at room temperature to quantitatively yield the starting nickel hydride dimer and free biphenyl (eq 3). Unlike other homogeneous systems, no

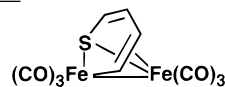


hydride, proton, or hydrogen atom source is required for desulfurization, only in the release of free biphenyl. Similar reactivity has been observed with alkylated dibenzothiophenes and analogous Pt complexes.

The novel reactivity of the nickel system and its equally unique desulfurization chemistry prompted Jones to expend considerable effort to elucidate mechanistic details. Isolation, structural characterization, and independent synthesis of each of the organometallic products in eq 2 as well as other subsidiary reaction products has allowed Jones to propose a complete reaction mechanism.<sup>16–18</sup> One of the key reaction steps involves formation of a bimetallic DBT-bridged complex, characterized by insertion of one metal center into a S–C bond of the DBT and coordination of a second metal center to the sulfur atom and olefinic portion of the central ring system (see Chart 1 for examples). Unfortunately, Jones has not been able to detect the dinickel DBT-bridged complex spectroscopically, but he proposes its existence based on bridged adducts observed for T and BT analogues. Other reports of thiophene-bridged complexes can be found throughout the HDS literature. Examples containing virtually every group 8–10 transition metal and a wide variety of chalcogen-containing heterocycles are known.<sup>19</sup> Chart 1 provides structural examples and illustrates the metals and heterocycles from which bridged adducts are

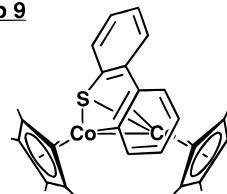
Chart 1

## Group 8



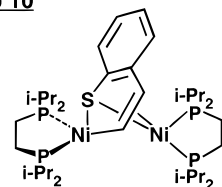
Fe: T, BT,<sup>20–22</sup>  
2-MeT, 3-MeT,<sup>23</sup>  
Se,<sup>24</sup> BTe<sup>9</sup>  
Ru: BT,<sup>25</sup> BTe<sup>9</sup>  
Os: Se, Te,<sup>24,26</sup> BT<sup>27</sup>

## Group 9

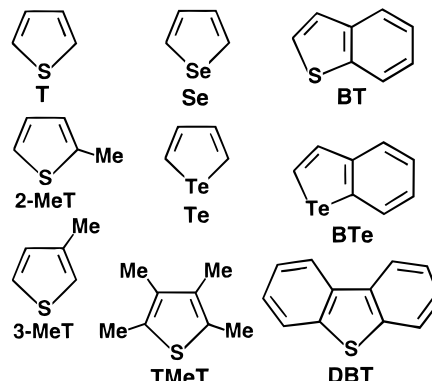


Co: T, BT, DBT<sup>28–31</sup>  
Rh: TMeT<sup>32</sup>  
Ir: T<sup>12</sup>

## Group 10



Ni: T, BT<sup>16</sup>  
Pd: T, BT<sup>31</sup>



known to form.<sup>8,9,12,20–33</sup> Although coordination complexes of this type have been known since 1960 when a benzothiaferrole was reported by King and Stone,<sup>20–22,34</sup>

(19) One example of a dirhenium BT-bridged complex has been reported. Angelici, R. J.; Reynolds, M. A.; Guzei, I. A. In *Transition Metal Complexes of W, Mo, Cr, Re, and Mn as Models for the Adsorption and Activation of Thiophene, Benzothiophene, and Dibenzothiophene on HDS Catalysts*; Angelici, R. J., Reynolds, M. A., Guzei, I. A., Eds.; Boston, MA, 1999.

(20) Kaesz, H. D.; King, R. B.; Manuel, T. A.; Nichols, L. D.; Stone, F. G. A. *J. Am. Chem. Soc.* **1960**, *82*, 4749–4750.

(21) King, R. B.; Stone, F. G. A. *J. Am. Chem. Soc.* **1960**, *82*, 4557–4562.

(22) King, R. B.; Treichel, P. M.; Stone, F. G. A. *J. Am. Chem. Soc.* **1961**, *83*, 3600–3604.

(23) Hübener, P.; Weiss, E. *J. Organomet. Chem.* **1977**, *129*, 105–115.

(24) Arce, A. J.; Machado, R.; Rivas, C.; Santis, Y. D. *J. Organomet. Chem.* **1991**, *419*, 63–75.

(25) Arce, A. J.; Santis, Y. D.; Karam, A.; Deeming, A. J. *Angew. Chem., Int. Ed. Engl.* **1994**, *33*, 1381–1383.

(26) Arce, A. J.; Deeming, A. J.; Santis, Y. D.; Machado, R.; Manzur, J.; Rivas, C. *J. Chem. Soc., Chem. Commun.* **1990**, 1568–1569.

(27) Arce, A. J.; Karam, A.; Santis, Y. D.; Capparelli, M. V.; Deeming, A. J. *Inorg. Chim. Acta* **1999**, *285*, 277–282.

(28) Jones, W. D.; Chin, R. M. *Organometallics* **1992**, *11*, 2698–2700.

(29) Jones, W. D.; Chin, R. M. *J. Organomet. Chem.* **1994**, *472*, 311–316.

(30) Jones, W. D.; Vici, D. A.; Chin, R. M.; Roache, J. H.; Myers, A. W. *Polyhedron* **1997**, *16*, 3115–3128.

(31) Jones, W. D. Personal communication.

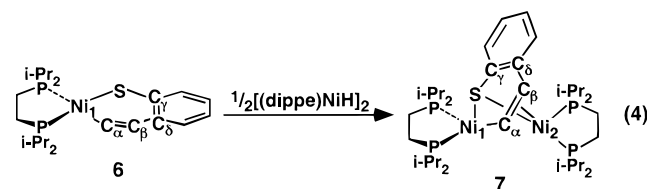
(32) Lou, S.; Skaugset, A. E.; Rauchfuss, T. B.; Wilson, S. R. *J. Am. Chem. Soc.* **1992**, *114*, 1732–1735.

(17) Vici, D. A.; Jones, W. D. *J. Am. Chem. Soc.* **1997**, *119*, 10855–10856.

(18) Vici, D. A.; Jones, W. D. *J. Am. Chem. Soc.* **1999**, *121*, 4070–4071.

neither their general electronic properties nor their possible role in homogeneous desulfurization reactions has been fully investigated. This lack of inquiry prompted us to undertake a detailed study of bimetallic thiophene-bridged complexes to ascertain information on bonding, S–C bond activation, complex formation and stability, and ultimately their role in the desulfurization of Jones's nickel system.

We examined several dinuclear thiophene-bridged complexes, including  $[(\text{CO})_3\text{Fe}]_2(\eta\text{-3-MeT})$ ,<sup>23</sup>  $[(\text{Cp}^*)_2\text{Co}]_2(\eta\text{-X})$  ( $\text{X} = \text{T}, \text{BT}, \text{DBT}$ ),<sup>28–31</sup>  $[(\text{CO})_3\text{Ru}]_2(\eta\text{-BT})$ ,<sup>25</sup> and  $[(\text{dippe})\text{Ni}]_2(\eta\text{-BT})$ .<sup>16</sup> Since we found little variance in the bonding interactions in the different complexes, we limit our report here principally to  $[(\text{dippe})\text{Ni}]_2(\eta\text{-BT})$  (see Chart 1). Discussion of this specific complex is convenient since both the parent  $d^8$  square-planar transition-metal-inserted complex  $(\text{dippe})\text{Ni}(\eta^2\text{-S,C-BT})$  (**6**) and the bridged adduct  $[(\text{dippe})\text{Ni}]_2(\eta\text{-BT})$  (**7**) have been structurally characterized (eq 4). Studying these

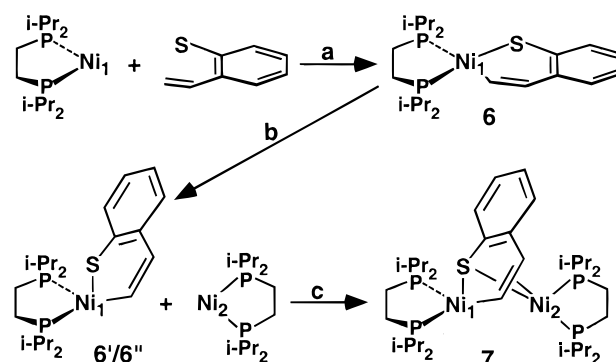


two complexes together simplifies the bonding description in **7** and allows us to describe how a second  $[(\text{dippe})\text{Ni}]$  fragment bonds to **6** to form the bridged adduct **7**, what effects coordination of the second metal has on the metal–ligand bonds of **6**, and what factors affect the stability of **7**. Discussion of the bonding in **7** also allows us to comment on the existence and role of a DBT-bridged analogue in the chemistry shown in eq 2. The ideas we present here are easily extended to other bridged systems.

## Results and Discussions

**Bonding in  $(\text{dippe})\text{Ni}(\eta^2\text{-S,C-BT})$  (**6**) and  $[(\text{dippe})\text{Ni}]_2(\eta\text{-BT})$  (**7**).** Examination of the structure of **6** shows that the  $[(\text{dippe})\text{Ni}]$  fragment ( $\text{Ni}_1$ ; see eq 4 for the labeling scheme used throughout this report) is inserted into the S–C<sub>vinyl</sub> bond of benzo[*b*]thiophene. The geometry around the nickel is square-planar, and the whole of the metallacycle lies in the plane of the four metal–ligand bonds; that is, the molecule possesses near- $C_s$  symmetry. When a second  $[(\text{dippe})\text{Ni}]$  fragment ( $\text{Ni}_2$ ) coordinates to **6** to form the BT-bridged complex **7**, the square-planar coordination geometry of  $\text{Ni}_1$  becomes slightly distorted, and the metallathiacycle bends sharply along the S/C<sub>α</sub> axis. The second nickel center ( $\text{Ni}_2$ ) binds in a tetrahedral arrangement to the sulfur atom and C<sub>α</sub>–C<sub>β</sub> double bond of the central ring system. Coordination of  $\text{Ni}_2$  also leads to an increase in the  $\text{Ni}_1$ –S bond distance from 2.131 to 2.263 Å and a contraction of the S–Ni–C<sub>α</sub> bond angle from 94.8° to

Scheme 1



88.5° (the  $\text{Ni}_1$ –C<sub>α</sub> bond distance is unaffected) and positions the S and C<sub>α</sub> atoms essentially equidistant between the two nonbonding metal centers ( $\text{Ni}_1$ – $\text{Ni}_2$  distance = 2.704 Å). Given the  $C_1$  symmetry of **7**, it is not surprising that the molecular orbital calculations on the complex are plagued with complicated orbital mixing and are difficult to interpret. Description of the bonding, however, is facilitated by separating the complex into its three component fragments, two  $[(\text{dippe})\text{Ni}]$  fragments and one “opened” BT fragment, and then examining their individual interactions. This involves describing the interactions surrounding the insertion of  $[(\text{dippe})\text{Ni}]$  into BT to form **6** (Scheme 1, step a), discussing the effects on the electronic structure on going from the planar complex **6** to a bent complex **6/6''** (Scheme 1, step b), and, finally, examining the interactions between a “distorted”  $[(\text{dippe})\text{Ni}]$ -inserted-BT and a second  $[(\text{dippe})\text{Ni}]$  fragment to form **7** (Scheme 1, step c). While this approach certainly has its limits, it does provide the details, which are otherwise obscured, required to fully describe the bonding interactions in the complex.

The energy level diagram for the square-planar,  $[(\text{dippe})\text{Ni}]$ -inserted-BT complex **6** is shown in Figure 1. The fragment molecular orbitals for  $[(\text{dippe})\text{Ni}]$ , typical of an  $\text{ML}_2$  fragment,<sup>35</sup> are shown on the left of the figure. The orbitals are filled through the  $d_{x^2-y^2}$  for the  $d^{10}$  nickel. It is important to recognize that both the  $a_1$  and “ $p_z$ ” orbitals are stabilized with respect to an octahedral field by loss of  $\sigma$  antibonding interactions and can therefore play an integral role in metal–ligand bonding. The ligand orbitals, shown on the right of Figure 1, are characteristic of other opened benzothiophene fragments previously reported;<sup>36</sup> the five frontier orbitals include C<sub>α</sub>–C<sub>β</sub>  $\pi/\pi^*$  orbitals, S–C<sub>α</sub>  $\sigma/\sigma^*$  orbitals (SHOMO/LUMO), and a S  $\pi$  lone-pair orbital (HOMO). Combining the  $[(\text{dippe})\text{Ni}]$  and opened BT fragment molecular orbitals generates the complete energy level diagram for **6**. While the interactions are similar to other metal-inserted-thiophene complexes we have studied,<sup>36</sup> a few points are worth emphasizing. First, the metal–BT  $\sigma$  bonds form from interactions between combinations of the metal  $a_1$  and  $d_{x^2-y^2}$  fragment orbitals and combinations of the ligand SHOMO and LUMO. The interactions lead to a formal, two-electron oxidation of  $\text{Ni}_1$ . The square-planar geometry

(33) Bacchi, A.; Bianchini, C.; Herrera, V.; Jiménez, M. V.; Mealli, C.; Meli, A.; Moneti, S.; Peruzzini, M.; Sánchez-Delgado, R. A.; Vizza, F. *J. Chem. Soc., Chem. Commun.* **1995**, 921–922.

(34) Interestingly, the thiaferrole they discovered was the first metal-inserted thiophene complex, the first example of a bimetallic thiophene-bridged species, and the first instance of desulfurization of thiophene by a soluble metal complex.

(35) Albright, T. A.; Burdett, J. K.; Whangbo, M. H. *Orbital Interactions in Chemistry*; Wiley: New York, 1985.

(36) Palmer, M.; Carter, K.; Harris, S. *Organometallics* **1997**, *16*, 2448–2459.



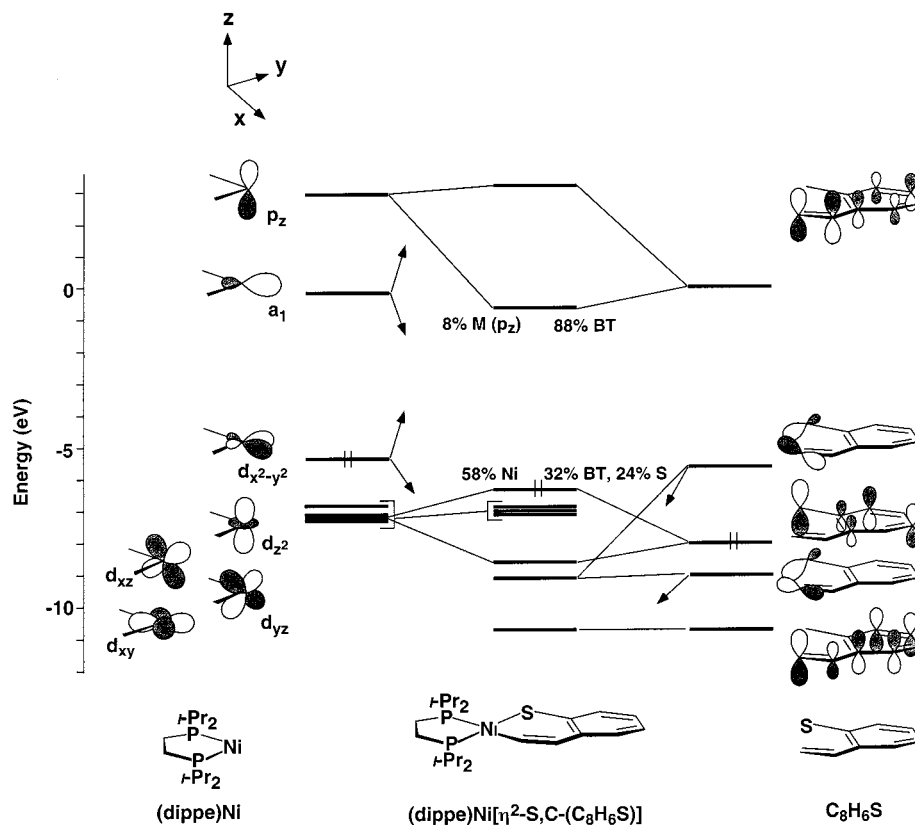


**Figure 1.** Calculated energy level diagrams for (dippe)Ni( $\eta^2$ -S,C-SC<sub>8</sub>H<sub>6</sub>) and for the (dippe)Ni and opened benzothiophene fragments.

is consistent with a  $d^8$  nickel. Second, the metal  $d_{yz}$  fragment orbital and BT HOMO participate in a two-orbital/four-electron interaction. The antibonding combination is the HOMO of **6** and contains a significant contribution from the sulfur  $\pi$  lone-pair orbital. Third, the metal  $p_z$  orbital mixes with the BT SLUMO to form the LUMO of **6**. Because the BT SLUMO lies lower in energy than the  $p_z$  orbital, the LUMO of the complex is composed primarily of the BT SLUMO (88%). This is in contrast to other similar  $d^8$  square-planar metal-inserted-thiophene complexes which were found to contain metal-based LUMOs;<sup>36</sup> we return to the significance of this later.

Bending the heterocycle of **6** is a necessary step in the formation of **7** (see Scheme 1). Although this is surely a dynamic process, it is useful to compare the bonding in an isolated bent ring system to the bonding in **6** and determine whether distortion of the heterocycle, lengthening of the Ni<sub>1</sub>–S distance, and contraction of the S–Ni<sub>1</sub>–C <sub>$\alpha$</sub>  angle on going from **6** to **7** are due to electronic factors. Two different models were studied to answer these questions. One of the models (**6'**) was constructed by artificially inducing a bend in the heterocycle of **6**; the structure of the other model (**6''**) was taken directly from the [(dippe)Ni<sub>1</sub>]-inserted-BT moiety of **7**. The structures of the two models differ principally in the Ni<sub>1</sub>–S distance and S–Ni<sub>1</sub>–C <sub>$\alpha$</sub>  angle. Our results show that the bonding interactions and the characters of the orbitals in **6'** and **6''** do not differ significantly from those in **6**. The strengths of the Ni<sub>1</sub>–S and Ni<sub>1</sub>–C <sub>$\alpha$</sub>  bonds decrease when the heterocycle is bent, but a comparison of bond orders (Table 1, column 1) shows that the changes are quite small. The decrease

**Table 1.** Calculated Bond Orders of the Ni<sub>1</sub>–S and Ni<sub>1</sub>–C <sub>$\alpha$</sub>  Bonds of **6**, **6'**, and **6''**

	bond order	
	Ni <sub>1</sub> –S	Ni <sub>1</sub> –C <sub><math>\alpha</math></sub>
<b>6</b>	0.697	0.815
<b>6'</b>	0.662	0.805
<b>6''</b>	0.641	0.797

is largest for the Ni<sub>1</sub>–S bond in **6''**, where the bond distance increases by 0.13 Å. The similar M–X bond strengths in the planar and bent ring structures are not entirely unexpected, since bending the ring does not significantly alter the  $\sigma$  interactions responsible for the M–X bonds<sup>37</sup>

On the basis of solely the Ni<sub>1</sub>–X bonding interactions found in **6**, **6'**, and **6''** one could conclude that formation of **7** via coordination of the second [(dippe)Ni] fragment directly to the *planar* **6** should be favored, since **6** does possess the strongest Ni<sub>1</sub>–S and Ni<sub>1</sub>–C <sub>$\alpha$</sub>   $\sigma$  bonds. (While the effect of bonding the second nickel center to the BT moiety should be considered in this argument, Ni<sub>2</sub> interacts only with BT  $\pi$  orbitals (see below) and should not significantly affect the Ni<sub>1</sub>–X  $\sigma$  bond strengths.) Simply bending **6**, without changing the Ni<sub>1</sub>–S distance and S–Ni<sub>1</sub>–C <sub>$\alpha$</sub>  angle, also provides for better Ni<sub>1</sub>–X bonding interactions than the actual [(dippe)Ni<sub>1</sub>]-inserted-BT moiety (**6''**) of **7**. These results, coupled with space-filling models, suggest that geometry changes observed in **7** are primarily due to steric interactions between the bulky isopropyl groups on the two [(dippe)Ni] fragments. Rearrangement of the BT moiety provides maximum

(37) Blonski, C.; Myers, A. W.; Palmer, M.; Harris, S.; Jones, W. D. *Organometallics* **1997**, *16*, 3819–3827.

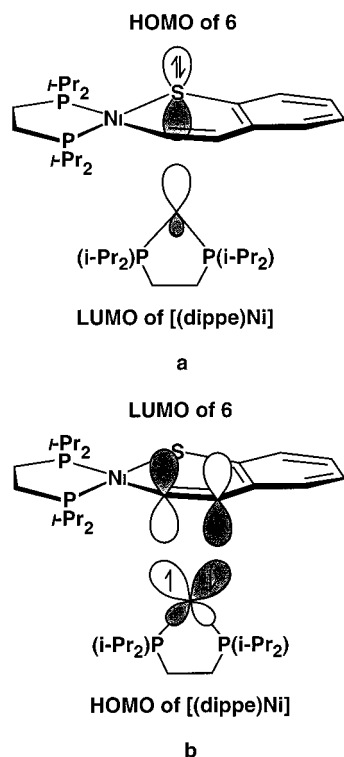


**Figure 2.** Idealized representations of the bonding interactions between the frontier orbitals of the planar, metal-inserted complex **6** and a second [(dippe)Ni] fragment: (a) the interaction between the HOMO of **6** and the LUMO of the [(dippe)Ni] fragment; (b) the interaction between the LUMO of **6** and the HOMO of the [(dippe)Ni] fragment.

separation between the metal fragments while maintaining metal–BT bonding. Separation between the two metal fragments is readily achieved due to the absence of a Ni<sub>1</sub>–Ni<sub>2</sub> bond (2.704 Å) and is enhanced by both ring contraction and Ni<sub>1</sub>–S bond lengthening.

Given the above discussion, characterization of the bonding in **7** is relatively straightforward. Consequently, we have chosen to give a more qualitative description of the bonding, rather than inundate the reader with the intricacies of the complete energy level diagram. The second nickel center (Ni<sub>2</sub>) binds to the sulfur atom and C<sub>α</sub>–C<sub>β</sub> double bond of the central ring system (eq 4). The Ni<sub>2</sub>–S  $\sigma$  bond is formed from the sulfur  $\pi$  lone-pair HOMO of **6**' and the LUMO of [(dippe)Ni] (Figure 2a). The large energy difference between these two orbitals (~7 eV) results in a fairly weak interaction, reflected in a calculated bond overlap population of only 0.131. In comparison, the Ni<sub>1</sub>–S bond overlap population is calculated to be 0.353. The bonding between Ni<sub>2</sub> and the olefinic bond of the heterocycle is best described as classical Dewar–Chatt–Duncanson  $\sigma$ -bonding/ $\pi$ -back-bonding.<sup>38,39</sup> The  $\sigma$ -bonding interaction involves forward donation from the olefin  $\pi$  bond of the metallacycle into the LUMO of the [(dippe)Ni] fragment. This interaction is relatively weak, however, due to large energy separations and poor directional properties of the orbitals involved. The  $\pi$  back-bonding interaction involving transfer of electron density from the metal fragment HOMO ( $d_{x^2-y^2}$ ) into the olefin  $\pi^*$  orbital (LUMO of **6**') is more extensive (Figure 2b). The magnitude of the

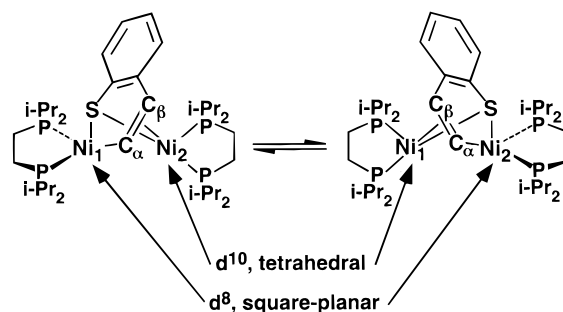


**Figure 3.** "Flip-flop" of the  $\eta^2$ -coordinated double bond observed in **7**. The fluxionality in the ring system is accompanied by a transfer of a pair of electrons between the two nickel centers and a change in coordination geometry of each metal.

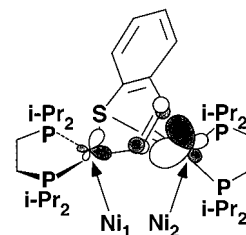


**Figure 4.** Idealized representation of the molecular orbital responsible for shuttling a pair of electrons between the two nickel centers of **7** during the "flip-flop" of the  $\eta^2$ -coordinated double bond. The electrons are initially localized on Ni<sub>2</sub>.

$\pi$ -back-bonding is reflected in the population of the previously empty LUMO of **6**' by 0.49 electrons and an increase in the C<sub>α</sub>–C<sub>β</sub> bond distance (1.340 Å in **6** vs 1.372 Å in **7**). (Similar differences in the strength of metal–olefin  $\sigma$  bonding and  $\pi$  back-bonding interactions have also been observed in calculations on mononuclear,  $\eta^3$ -bound thiophene complexes containing both M–S and M–olefin bonds.)<sup>40</sup> In all, neither bonding mechanism is very efficient; the bond overlap populations of the Ni<sub>2</sub>–C<sub>α</sub> and Ni<sub>2</sub>–C<sub>β</sub> bonds are 0.160 and 0.057, respectively. Formal oxidation of Ni<sub>2</sub> is not observed in the calculation. The tetrahedral geometry is consistent with a d<sup>10</sup> nickel.

The ring system of **7** (and other bimetallic thiophene-bridged complexes)<sup>3,28,30</sup> is known to be fluxional in solution.<sup>16</sup> The process simply involves a "flip-flop" of the  $\eta^2$ -coordinated double bond from one metal center to the other (Figure 3). The change in ring geometry is also accompanied by a transfer of a pair of electrons between the metal centers and a change in the geometry around each metal. For example, the fluxionality of **7** results in a reversal in the oxidation states (0  $\leftrightarrow$  +2) and geometries (tetrahedral  $\leftrightarrow$  square-planar) of the two nickel centers. The fluxionality most likely stems from the weak Ni<sub>2</sub>–C<sub>β</sub> interaction. The fluxional behavior would not be possible, however, without a convenient mechanism to shuttle the electrons back and forth between the metal centers. Our calculations show that the molecular orbital responsible for electron transfer is the Ni<sub>2</sub>–carbon  $\pi$  back-bonding orbital. Initially, the electrons in the orbital are localized on Ni<sub>2</sub> (Figure 4). As C<sub>β</sub> begins to shift from Ni<sub>2</sub> to Ni<sub>1</sub>, the electrons move out into the ring system and eventually end up localized

(38) Chatt, J.; Duncanson, L. A. *J. Chem. Soc.* **1953**, 2939–2947.

(39) Dewar, M. J. S. *Bull. Soc. Chim. Fr.* **1951**, 18, C79.

(40) Kirsch, J. E.; Harris, S. Manuscript in preparation.

**Table 2. Bond Distances and Bond Overlap Populations between the Atoms in the Central Ring System of the Metallathiacycles of **6** and **7****

	bond length, Å			bond overlap population		
	<b>6</b>	<b>7</b>	$\Delta(7-6)$	<b>6</b>	<b>7</b>	$\Delta(7-6)$
Ni–S	2.131	2.263	+0.132	0.424	0.353	–0.071
S–C <sub>γ</sub>	1.758	1.752	–0.006	0.823	0.868	+0.045
C <sub>γ</sub> –C <sub>δ</sub>	1.388	1.409	+0.021	1.114	1.183	+0.069
C <sub>δ</sub> –C <sub>β</sub>	1.430	1.466	+0.036	0.941	0.981	+0.040
C <sub>β</sub> –C <sub>α</sub>	1.340	1.372	+0.032	1.320	1.183	–0.137
C <sub>α</sub> –Ni	1.911	1.908	–0.003	0.518	0.507	–0.011

on Ni<sub>1</sub>. Ni<sub>2</sub> is formally oxidized by two electrons during the process and becomes square-planar; Ni<sub>1</sub> is reduced by two electrons and becomes tetrahedral. Evidence that the electrons migrate between the metal centers through the ring system can be obtained by calculating the transition state (TS) between the two conformers; that is, charges on the ring atoms should be more negative at the TS. Because determining the TS for **7** is computationally expensive, we instead calculated the TS between the two conformers of a less-demanding diiron thiophene-bridged complex [(CO)<sub>3</sub>Fe]<sub>2</sub>(η-T). As expected, the charge of the ring atoms are found to be more negative at the TS, suggesting that the electrons do indeed migrate between the two metals through the ring system.

This full picture of the bonding in **7** enables us to comment on whether coordination of a second metal center to **6** leads to Ni<sub>1</sub>–S, Ni<sub>1</sub>–C<sub>α</sub>, and/or S–C bond activation. Table 2 displays the bond lengths and bond overlap populations between all of the atoms in the central ring system of the metallathiacycles of both **6** and **7**. Although the Ni<sub>1</sub>–S bond is lengthened by 0.13 Å upon coordination, bond overlap population analysis suggests that the bond is not significantly weakened. This results from the σ nature of the Ni<sub>1</sub>–S bond; the contraction of the S–Ni–C<sub>α</sub> angle re-establishes the orbital overlap between the metal and sulfur and diminishes the effect of the increased distance. Coordination also has little effect on the S–C<sub>γ</sub> and Ni<sub>1</sub>–C<sub>α</sub> bond. The only bond significantly weakened is the C<sub>α</sub>–C<sub>β</sub> double bond which stems from occupation of the π\* orbital. These results suggest that coordination of a second metal center does not, by itself, directly lead to bond-breaking reactions.

**Stability of Bimetallic Thiophene-Bridged Adducts Derived from Square-Planar Transition-Metal-Inserted Complexes.** While numerous square-planar, transition-metal-inserted thiophene complexes have been reported in the past few years,<sup>16,17,41–45</sup> only a handful have been shown to form bimetallic thiophene-bridged species. All of the known examples are based on Jones's [(dippe)M] system. He has reported spectroscopic evidence for [(dippe)Ni]<sub>2</sub>(η-T),<sup>16</sup> [(dippe)Ni]<sub>2</sub>(η-BT),<sup>16</sup> [(dippe)Pd]<sub>2</sub>(η-T),<sup>31</sup> and [(dippe)Pd]<sub>2</sub>(η-BT)<sup>31</sup> and has confirmed the assignments by structural charac-

terization of [(dippe)Ni]<sub>2</sub>(η-BT). Surprisingly, no dinuclear DBT-bridged complex containing Ni, Pd, or Pt and no diplatinum species of any kind have been detected.

The bonding in **7** provides clues to why certain thiophene-bridged complexes have not been observed. Idealized representations of the two interactions principally responsible for the bonding in **7** are shown in Figure 2 for the planar **6** and the coordinating metal fragment. The Ni<sub>2</sub>–S σ bond results from interactions between the metal fragment LUMO and the HOMO of **6** (Figure 2a), while the Ni<sub>2</sub>–carbon bonds stem primarily from back-bonding interactions between the metal fragment HOMO and the C<sub>α</sub>–C<sub>β</sub> π\* LUMO of **6** (Figure 2b). Any factor that decreases the overlap between these frontier orbitals should decrease the thermodynamic stability of a bridged adduct. To better understand the role of orbital overlap in the formation of dinuclear thiophene-bridged complexes, we performed a series of calculations on both ML<sub>2</sub> fragments and square-planar, transition-metal-inserted thiophene complexes. Different components of the two substrates (e.g., metal, ligand, etc.) were varied systematically in order to examine how these changes influence the overlap and interactions between their frontier orbitals.

As might be expected, the character of the frontier orbitals of the ML<sub>2</sub> fragment is relatively unaffected by changes in the metal and/or phosphine ligands. Changes in the phosphine ligand also have little effect on the character and composition of the frontier orbitals of the square-planar metal-inserted complex and do not affect (electronically) the bonding interactions or the stability of a dinuclear thiophene-bridged species. The degree to which steric interactions between the metal-inserted precursor and the coordinating metal fragment affect complex stability are more difficult to quantify. Although Jones has suggested that his inability to observe a [(dippe)Ni]<sub>2</sub>(η-DBT) species may be due, in part, to unfavorable interactions between the DBT ligand and the bulky isopropyl groups on the dippe chelate of the coordinating metal fragment, molecular mechanics calculations predict that steric crowding is certainly not significant enough to preclude formation of a DBT-bridged adduct. Unfavorable interactions are mainly avoided by the ability of the thiophenic ligand to severely distort without adversely affecting metal–ligand bonding (see the bonding discussion for **7**). In fact, molecular rearrangement is so efficient that steric interactions may not significantly influence the lifetime of the DBT-bridged complex.

Unlike changes in the phosphine ligands, variations in the metal center and the thiophenic moiety do affect the composition of the frontier orbitals of a square-planar, metal-inserted complex. The most significant changes occur in the LUMO rather than HOMO of the complex. Although the character of the HOMO of the square-planar complex depends on the energy of the metal orbitals (the percentage of overall ligand character in the HOMO decreases as the energies of the metal orbitals increase), the sulfur contribution to the HOMO remains constant. Thus changes in the metal center have little effect on the overlap between the S-based HOMO and metal fragment LUMO (Figure 2a) and

(41) García, J. J.; Mann, B. E.; Adams, H.; Bailey, N. A.; Maitlis, P. M. *J. Am. Chem. Soc.* **1995**, *117*, 2179–2186.

(42) García, J. J.; Arevalo, A.; Capella, S.; Chehata, A.; Herdandez, M.; Montiel, V.; Picazo, G.; Del Río, F.; Toscano, R. A.; Adams, H.; Maitlis, P. M. *Polyhedron* **1997**, *16*, 3185–3195.

(43) Iretskii, A.; Adams, H.; García, J. J.; Picazo, G.; Maitlis, P. M. *Chem. Commun.* **1998**, 61–62.

(44) Arevalo, A.; Bernés, S.; García, J. J.; Maitlis, P. M. *Organometallics* **1999**, *18*, 1680–1685.

(45) Vicić, D. A.; Jones, W. D. *Organometallics* **1998**, *17*, 3411–3413.



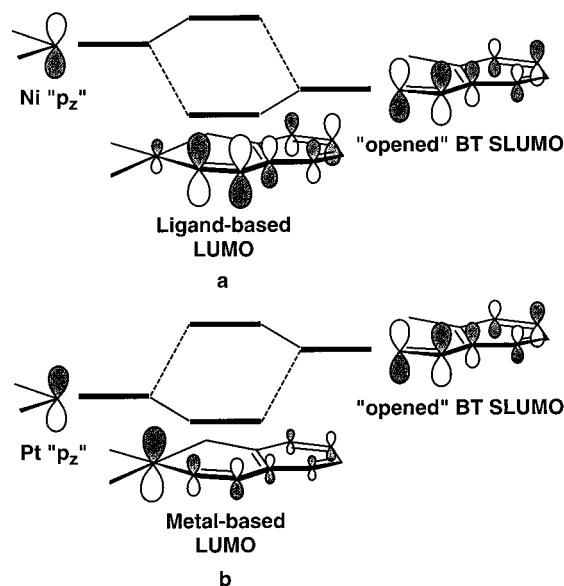


**Figure 5.** The effect different metals have on the character of the LUMO of square-planar transition-metal-inserted thiophene complexes. In part a, the high-energy nickel  $p_z$  orbital lies above the SLUMO of the opened BT, and the complex has a ligand-based LUMO. In part b, the lower energy platinum  $p_z$  orbital lies below the SLUMO of the opened BT, and the complex has a metal-based LUMO.

should not affect the stability of a bridged adduct. (Although the larger Pd or Pt atoms should overlap better with the sulfur than the smaller Ni, the difference is not expected to significantly influence the strength of the interaction.)

The LUMO of a square-planar complex such as **6** is a combination of the metal fragment  $p_z$  orbital and the SLUMO of the opened thiophene (e.g., see Figure 1). Changing the metal center leads to changes in the character of this LUMO which do have an effect on its overlap with the HOMO of the coordinating fragment (Figure 2b) and thus the stability of the bridged adduct. For a first-row transition metal, such as Ni, the metal orbitals are high enough in energy that the  $p_z$  orbital actually lies above the SLUMO of the opened BT. This results in a LUMO in the square-planar complex that is dominated by ligand character (>80%), with large contributions from  $C_\alpha$  and  $C_\beta$  (Figure 5a). For a third-row transition metal, like platinum, the metal fragment orbitals are low enough in energy that the  $p_z$  orbital lies below the ligand SLUMO. The shift in orbital energies results in a LUMO with markedly less ligand character (<50%), substantial reductions in the orbital coefficients of  $C_\alpha$  and  $C_\beta$  (Figure 5b), and poorer overlap with the HOMO of the coordinating metal fragment. These trends clearly indicate that the stability of a dinickel thiophene-bridged complex should be enhanced over a di-Pd or -Pt thiophene-bridged analogue.

The nature of the thiophene ligand (T, BT, or DBT) also influences the character of the LUMO of the square-planar complex and, ultimately, the stability of thiophene-bridged complexes. Jones has suggested that his inability to observe a dinickel DBT-bridged species may be partly due to the lack of "isolated"  $C_\alpha$ – $C_\beta$  double-bond character in **1**. The argument is qualitatively based on the idea that a pure, localized double bond is necessary in order to effectively interact with the

**Table 3.** Lengths and Overlap Populations of the  $C_\alpha$ – $C_\beta$  Bond in Square-Planar Transition-Metal-Inserted Thiophene Complexes (Whether a Bridged Adduct Is Known to Form from the Parent Metal-Inserted Complex Is Noted)

	bond length, Å	bond overlap population	bimetallic bridged complex observed?
(dippe)Ni( $\eta^2$ -S,C-T) <sup>16</sup>	1.363	1.286	yes
(dippe)Ni( $\eta^2$ -S,C-BT) <sup>16</sup>	1.340	1.320	yes
(dippe)Ni( $\eta^2$ -S,C-DBT) <sup>17</sup>	1.416	1.151	no
(dippe)Pd( $\eta^2$ -S,C-T) <sup>31</sup>	<i>a</i>	<i>a</i>	yes
(dippe)Pd( $\eta^2$ -S,C-BT) <sup>31</sup>	<i>a</i>	<i>a</i>	yes
(dippe)Pd( $\eta^2$ -S,C-DBT) <sup>31</sup>	1.414	1.125	no
(Et <sub>3</sub> P) <sub>2</sub> Pt( $\eta^2$ -S,C-3-MeT) <sup>42</sup>	1.329	1.334	no
(Et <sub>3</sub> P) <sub>2</sub> Pt( $\eta^2$ -S,C-BT) <sup>41</sup>	1.340	1.343	no
(Et <sub>3</sub> P) <sub>2</sub> Pt( $\eta^2$ -S,C-DBT) <sup>42</sup>	1.429	1.147	no
(dippe)Pt( $\eta^2$ -S,C-DBT) <sup>31</sup>	1.399	1.182	no

<sup>a</sup> No structure has been determined from crystallographic methods.

coordinating metal fragment. A more localized double bond should correlate with a shorter bond length and a larger calculated bond overlap population. Comparisons of these two quantities for several square-planar, transition-metal-inserted complexes (Table 3) indicate that  $C_\alpha$ – $C_\beta$  double-bond character follows the trend BT > T  $\gg$  DBT; stability of dinuclear bridged adducts should follow the same trend. Indeed, Jones finds that stability in his dinickel systems follows BT > T  $\gg$  DBT. Rauchfuss has observed an identical trend for thiaferroles having the formula [(CO)<sub>3</sub>Fe]<sub>2</sub>( $\eta$ -X); X = BT > T  $\gg$  DBT.<sup>8</sup> The result also correlates well with the fact that only T- and BT-bridged species have been reported to form from square-planar, metal-inserted complexes (Table 3, column 3). On a more fundamental level, the difference between DBT and the other two heterocycles is the delocalization of the molecular orbitals of DBT caused by fusing a phenyl group to the  $C_\alpha$ – $C_\beta$  bond. This leads to smaller orbital coefficients on  $C_\alpha$  and  $C_\beta$  and a smaller contribution of the  $C_\alpha$ – $C_\beta$   $\pi^*$  orbital to the LUMO of the metal-inserted product. The result is poor overlap with the HOMO of the approaching metal fragment. Opened T and BT possess a more localized  $C_\alpha$ – $C_\beta$  double bond (one that is not part of an phenyl ring). The LUMO of the metal-inserted T/BT complex contains large orbital coefficients on  $C_\alpha$  and  $C_\beta$  and therefore is expected to overlap well with the HOMO of the coordinating metal fragment. This suggests that the stability of a T- or BT-bridged species should be enhanced over a DBT-bridged analogue.

In summary, the dominant factor determining the stability of the bimetallic thiophene-bridged complexes appears to be the strength of the interaction between the LUMO of the metal-inserted thiophene and the HOMO of the metal fragment. The overlap between these two orbitals is mainly influenced by the  $C_\alpha$ – $C_\beta$  character of the LUMO of the metal-inserted complex, which depends greatly on the metal center and the thiophenic ligand. Our results show that the  $C_\alpha$ – $C_\beta$  character in the LUMO decreases in the order Ni > Pd > Pt and T  $\approx$  BT  $\gg$  DBT. The trends suggest that, within group 10, complexes containing Ni and/or T/BT should form the most stable bridged adducts, while those containing Pt and/or DBT should be least stable. This correlates well with experimental observations of bridged complexes derived from square-planar transi-

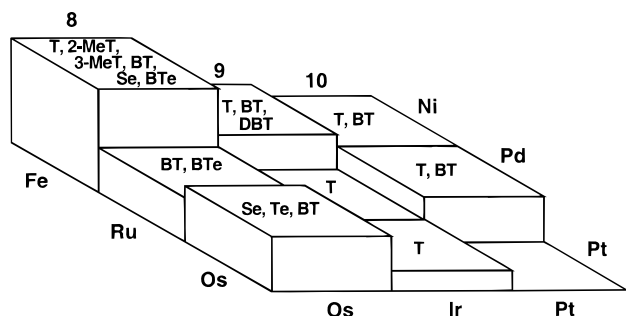


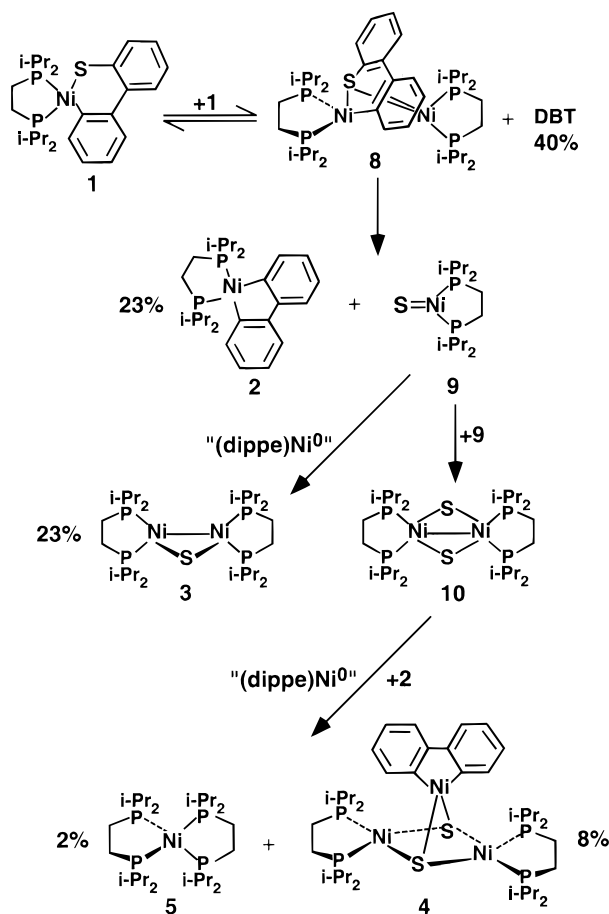
**Figure 6.** Display of the relative abundances of bimetallic heterocycle-bridged complexes for group 8, 9, and 10 transition metals. Chart 1 serves as a key to the heterocycle abbreviations and provides structural examples.

tion-metal-inserted thiophene complexes (see Table 3, column 3). Calculations on a number of thiophene-bridged complexes containing group 8 and 9 metals reveal similar trends; that is, metal-inserted complexes containing earlier, first-row transition metals and/or T/BT should interact more effectively with a coordinating metal fragment and form more stable bridged adducts than those complexes containing later, third-row transition metals and/or DBT. Correlation of our theoretical predictions with experimental observation is illustrated in Figure 6. The figure shows a comprehensive list of spectroscopically and structurally characterized bimetallic thiophene-, selenophene-, and tellurophene-bridged complexes. As predicted, diiron T/BT-bridged complexes are most abundant. Fewer complexes are observed upon moving across the periodic table and down a triad. No diplatinum-bridged species of any kind has been reported. The only DBT-bridged complex that has been observed forms from Co (an earlier, first-row transition metal).

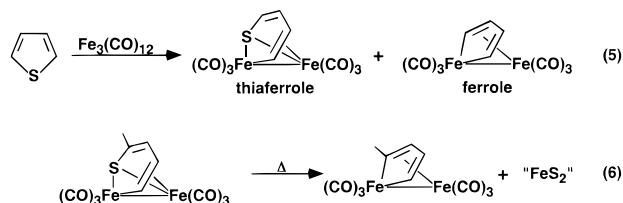
**Comments on the Existence of [(dippe)Ni]<sub>2</sub>( $\eta$ -DBT) (8).** Jones has proposed a mechanism<sup>16</sup> (Scheme 2) for the reaction shown in eq 2, which involves reversible loss of free DBT from the S–C insertion adduct **1** to generate reactive bisphosphine nickel(0) fragments. These fragments can then react further with remaining **1** to yield the bimetallic DBT-bridged complex **8**. Sulfur extraction from **8** produces one of the major products **2** (a metallacyclopentadiene) and the terminal sulfido nickel complex **9**. Reaction of **9** with a nickel(0) fragment generates the other major product **3**. Reaction of **9** with itself, followed by reaction with another nickel(0) fragment and **2**, produces both minor products. DBT accounts for 40% of the product mixture, **2** and **3** each account for 23%, and **4** and **5** comprise the balance of the product distribution.

One of the downsides of the mechanism is the lack of spectroscopic evidence for the DBT-bridged complex **8**. Our calculations provide an explanation for why a DBT-bridged adduct might be *thermodynamically* unstable, and there is no evidence indicating a lack of *kinetic* stability. Therefore, it seems reasonable that **8** could have a transient existence. The role of **8** in the reaction shown in eq 2 is also supported by several accounts in the literature that suggest that bimetallic thiophene-bridged complexes are precursors to metallacyclopentadienes such as **2**. For example, Stone and King described the isolation of both a thiaferrole (a diiron thiophene-bridged complex) and a ferrole (a metallacy-

**Scheme 2**



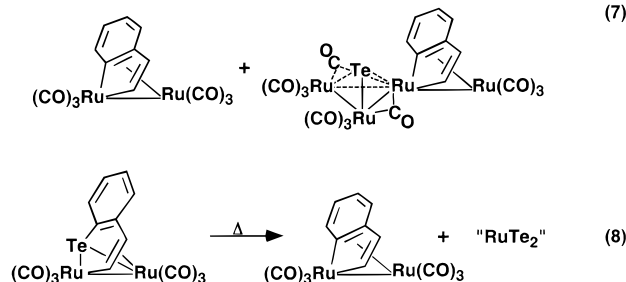
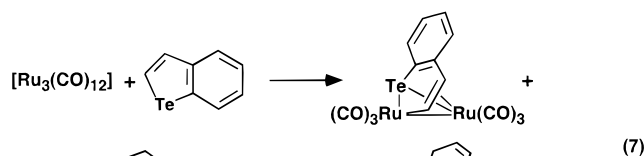
clopentadiene) from the reaction of thiophene with Fe<sub>3</sub>(CO)<sub>12</sub> (eq 5).<sup>16,20–22</sup> Hübener and Weiss later reported



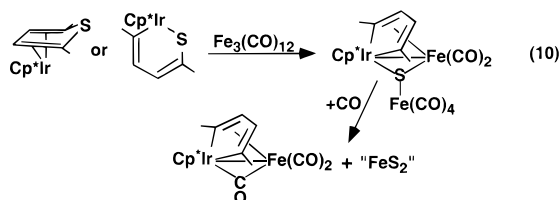
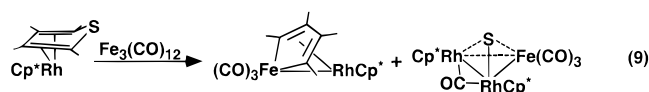
analogous products from the reaction of methylthiophenes with Fe<sub>3</sub>(CO)<sub>12</sub>.<sup>23</sup> They found that the thiaferrole could be directly converted to the ferrole by heating in refluxing benzene (eq 6). More recently, Arce and Deeming reported that the trinuclear carbonyl clusters Fe<sub>3</sub>(CO)<sub>12</sub>, Ru<sub>3</sub>(CO)<sub>12</sub>, Os<sub>3</sub>(CO)<sub>12</sub>, and Os<sub>3</sub>(CO)<sub>10</sub>(MeCN)<sub>2</sub> react with a number of sulfur, selenium, and tellurium heterocycles to give metallacyclopentadienes.<sup>9,24,25,46</sup> In several cases, bimetallic heterocycle-bridged species are also observed. Like the thiaferroles, the di-Fe, di-Ru, and di-Os BTe-bridged complexes directly yield metallacyclopentadienes simply by heating (eqs 7 and 8 provide representative examples).<sup>9</sup> Reactions of soluble metal–thiophene complexes with metal–carbonyl clusters are also known to produce metallacyclopentadienes. For instance, the reaction of Cp\*Rh( $\eta$ <sup>4</sup>-2,3,4,5-MeT) with Fe<sub>3</sub>(CO)<sub>12</sub> produces a mixed-metal metallacyclopentadiene and a trimetallic sulfur-capped cluster (eq 9),<sup>47</sup>

(46) Arce, A. J.; Arrojo, P.; Deeming, A. J.; Santis, Y. D. *J. Chem. Soc., Dalton Trans.* **1992**, 2424–2424.





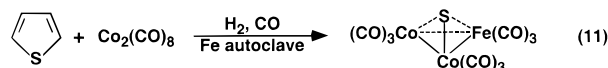
and reaction of  $\text{Cp}^*\text{Ir}(\eta^4\text{-2,5-MeT})$  or  $\text{Cp}^*\text{Ir}(\eta^2\text{-C,S-2,5-MeT})$  with  $\text{Fe}_3(\text{CO})_{12}$  forms a mixed-metal metallacyclopentadiene and a form of  $\text{FeS}_2$  or  $\text{Fe}_a\text{S}_b(\text{CO})_c$  (eq 10).<sup>48</sup>



Although no dinuclear thiophene-bridged complex has been observed for these last two examples, the presence of the metallacyclopentadiene structure in both reactions suggests a relationship to each of the other systems described above. The fact that the reactions shown in eqs 5–8 link dinuclear heterocycle-bridged species to metallacyclopentadienes suggests that all of the reactions, including eq 2, involve a bridged precursor.

**Comments on the Desulfurization of DBT.** The mechanism Jones proposes for the desulfurization of DBT (Scheme 2) is appealing because it utilizes the fact that deinsertion of  $(\text{dippe})\text{Ni}(0)$  from **1** is known to be facile,<sup>17</sup> it is consistent with release of 2 equiv of DBT, and it accounts for all four organometallic products. Unfortunately, neither the dinickel DBT-bridged complex **8** nor the terminal sulfido complex **9** has been directly observed. One other questionable feature of the mechanism is worth noting. Sulfur abstraction from **8** requires that **2** and **9** be formed in a 1:1 ratio. Examination of the full reaction mechanism (Scheme 2), therefore, demands that **2** make up 31% of the reaction mixture (23% directly as **2** and 8% in the form of **4**) and that **9** make up 39% of the reaction mixture (23% in the form of **3** and 16% in the form of **4**). Clearly, **2** and **9** are not formed in a 1:1 ratio. The difference in product distribution suggests that an additional process may be acting in concert with the mechanism shown in Scheme 2. We discuss a possibility below that is consistent with accounts in the literature and our calculational results.

As already mentioned, a common derivative of many dinuclear thiophene-bridged complexes is a metallacyclopentadiene species. The sulfur-containing product of such reactions is a "metal–sulfide." For the thiaferrole to ferrole reaction shown in eq 6, the sulfur-containing species was not determined but believed to be a form of  $\text{FeS}_2$ . Likewise, the chalcogen-containing species for the reactions shown in eq 8 and 10 were reported to be "RuTe<sub>2</sub>" and "FeS<sub>2</sub>", respectively. For the reaction shown in eq 9, the sulfur-containing species was found to be a trimetallic sulfur-capped cluster. A similar cluster was identified in the reaction of thiophene with the  $\text{Co}_2(\text{CO})_8$  dimer in an Fe autoclave (eq 11).<sup>49–51</sup> Unfortunately,



the hydrocarbon product was not identified. When all of these reaction are considered together, it is clear that there exists some similarity between these systems and the nickel desulfurization reaction. That is, dinuclear thiophene-bridged complexes lead to metallacyclopentadienes and metal–sulfide clusters. In the case of nickel, the metallacyclopentadiene is **2** and the "sulfur-capped cluster" is **3**. It is important to note that the clusters in eqs 9 and 11 are stable 48-electron, trimetallic clusters. In the nickel system, the total electron count and chelating phosphine ligands make it impossible to form a similar trimetallic cluster. Instead, the stable bimetallic "cluster" **3** forms.

A number of reactions reported by Arce and Deeming further link metallacyclopentadiene complexes to trimetallic sulfur-capped clusters.<sup>9</sup> For example, the reaction shown in eq 7 produces an adduct that appears to be a combination of the two species. Analogous products have been observed in other related systems. These products suggest that metallacyclopentadienes and sulfur-capped clusters may be formed from a common precursor. A possible mechanism for the desulfurization of DBT utilizing this assumption is shown in Scheme 3. As in Jones's proposed mechanism, the first step involves deinsertion of  $[(\text{dippe})\text{Ni}]$  from **1**; the  $\text{Ni}(0)$  fragment reacts with another molecule of **1** to form the DBT-bridged adduct. In the second step, rather than sulfur abstraction, a *third*  $[(\text{dippe})\text{Ni}]$  fragment binds to the sulfur atom to form a trimetallic intermediate. Several features of the electronic structure of **7** support attack at sulfur by an additional electrophilic metal fragment. First, the sulfur atom in **7** is  $\text{sp}^3$  hybridized. This results in the sulfur lone-pair orbital having good directional and spatial properties and leaves it easily accessible to an electrophile. In addition, the sulfur lone-pair orbital remains high in energy and, thus, reactive. Second, the charge on the sulfur atom is  $-0.29$ , making it attractive to an electrophilic metal. (For comparison, the charge of the sulfur atom of the parent metal-inserted complex **6** is  $-0.32$ .) Each of these features are possibly enhanced by the fluxionality of the ring system. Indeed, examination of the bridged complex  $[(\text{CO})_3\text{Fe}]_2(\eta\text{-T})$  shows that the sulfur lone-pair orbital becomes

(47) Lou, S. F.; Oglivy, A. E.; Rauchfuss, T. B.; Stern, C. L.; Wilson, S. R. *Organometallics* **1991**, 10, 1002.

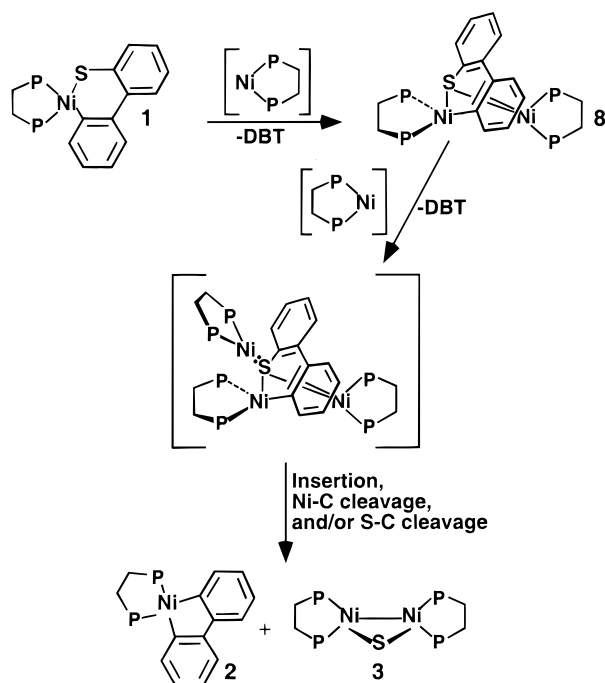
(48) Chen, J.; Daniels, L. M.; Angelici, R. J. *J. Am. Chem. Soc.* **1991**, 113, 2544–2552.

(49) Khatatb, S. A.; Markó, L.; Bor, G.; Markó, B. *J. Organomet. Chem.* **1964**, 1, 373–376.

(50) Natile, G.; Bor, G. *J. Organomet. Chem.* **1972**, 35, 185–193.

(51) Markó, L. *Gazz. Chim. Ital.* **1979**, 109, 247–.

Scheme 3



“more”  $sp^3$  hybridized, and the sulfur atom becomes more negatively charged at the TS state between the two conformers. Once the third [(dippe)Ni] fragment is coordinated to **8**, a number of different bond-breaking steps (insertion, Ni–C cleavage, S–C cleavage, etc.) can take place which will lead to the two major products.

Although desulfurization schemes requiring three transition metals are somewhat novel, a similar proposal has been made by Curtis and Druker.<sup>11,52</sup> While studying desulfurization reactions of the butterfly cluster  $Cp'_2Mo_2Co_2S_3(CO)_4$  ( $Cp' = C_5H_4Me$ ) with thiols, they proposed that a  $\mu^3$ -coordinated sulfur center “leads to activation of the S–C bond to homolytic cleavage by decreasing the bond dissociation energy by 20–25 kcal/mol”. They suggest that  $\mu^3$ -coordination produces a more stable sulfur-containing end-product (a  $\mu^3$ -coordinated sulfide vs an  $HS^\bullet$  radical) and allows the cluster to more easily cope with the oxidation that occurs on going from  $M_3(SR)$  to  $M_3(S)$ ; that is, the oxidation is spread out over the entire metal framework rather than localized on the sulfur atom. (A similar mechanism may be at play in the desulfurization reactions involving the ruthenium systems of Suzuki<sup>15</sup> and Shaver.<sup>53</sup>) It is reasonable, therefore, to suggest that the bond activation observed in Jones’s nickel system arises from similar factors. In other words, the role of the bimetallic DBT-bridged complex **8** may be to favor formation of a triply coordinated-sulfur intermediate, which then induces bond-breaking reactions.

### Summary

The Ni<sub>1</sub>–BT bonds in **6** are primarily derived from Ni–S and Ni–C $_{\alpha}$   $\sigma$  interactions. These interactions effectively oxidize the metal center, which leaves the

d,<sup>8</sup> Ni(+2) center in a square-planar environment. Coordination of an additional [(dippe)Ni] fragment produces a bend in the heterocycle of **6**. The distortion in the ring system has minimal effect on the electronic structure and metal–ligand bond strengths of **6**. Computational results and space-filling models both suggest that changes in ring geometry arise from steric rather than electronic factors. The second [(dippe)Ni] fragment coordinates to the sulfur atom through a  $\sigma$  bond to one of the S  $\pi$  lone pair orbitals of **6** and to the C $_{\alpha}$ –C $_{\beta}$  double bond of the metallathiacycle via a  $\sigma$ -bonding/ $\pi$ -back-bonding mechanism. Bond overlap population analysis indicates that each of these interactions is weak. (The weak Ni<sub>2</sub>–C $_{\beta}$  interaction contributes to the fluxionality that is observed in the ring system of **7**.) Of the three interactions, however, back-bonding into the C $_{\alpha}$ –C $_{\beta}$   $\pi^*$  orbital of **6** is the strongest. None of the interactions leads to a formal oxidation of Ni<sub>2</sub> and leaves the d,<sup>10</sup> Ni(0) center in a tetrahedral environment.

Calculations show that the thermodynamic stability of bimetallic thiophene-bridged adducts derived from square-planar transition-metal-inserted thiophene complexes is primarily dependent on the strength of the interaction between the LUMO of the metal-inserted thiophene and the HOMO of the coordinating metal fragment. The overlap between these two orbitals depends greatly on the nature of the metal center and the thiophenic ligand, and our results show that the strength of the interaction decreases in the order Ni > Pd > Pt and T  $\approx$  BT  $\gg$  DBT. This correlates well with experimental observations that show that, within group 10, Ni and/or T/BT are the most commonly observed bridged adducts, while those containing Pt and/or DBT are least commonly observed. Calculations on other thiophene-bridged complexes containing group 8 and 9 metals reveal similar trends; that is, metal-inserted complexes containing earlier, first-row transition-metals and/or T/BT interact more effectively with a coordinating metal fragment and form more stable bridged adducts than those complexes containing later, third-row transition metals and/or DBT.

Our calculations provide an explanation for why the dinickel DBT-bridged adduct **8** might be *thermodynamically* unstable and, therefore, difficult to detect spectroscopically. In addition, we find no evidence that supports an inherent kinetic instability. Consequently, like Jones, we believe that **8** plays an integral role in the desulfurization of DBT. The role of **8** in the reaction shown in eq 2 is also supported by several accounts in the literature that suggest that bimetallic thiophene-bridged complexes are precursors to metallacyclopentadienes such as **2**.

Minor discrepancies in the mechanism shown in Scheme 2 led us to propose an alternative pathway which may be acting in concert with Jones’s suggestion. Reports in the literature, coupled with the results of our calculational studies, suggest that the presence of a trimetallic intermediate in which a third [(dippe)Ni] fragment bonds to the sulfur atom of **8** is possible. Characteristics of the sulfur atom which might promote such an interaction, include a high-energy, easily accessible,  $sp^3$ -hybridized lone-pair orbital and relatively high negative charge. The fluxionality in the ring system of bimetallic adducts possibly enhances each of these

(52) Curtis, M. D.; Druker, S. H. *J. Am. Chem. Soc.* **1995**, *117*, 6366–6367.

(53) Shaver, A.; Mohammad, E.-K.; Lebus, A.-M. *Inorg. Chem.* **1999**, *38*, 5913–5915.

features; that is, the orbital properties of the lone-pair orbital should be improved and the charge on the sulfur atom should become increasingly negative at the TS between the two conformers. Once the trimetallic intermediate is formed, a number of different bond-breaking steps can lead to the two major products of the reaction. A desulfurization scheme requiring three transition metals has also been proposed by Curtis and Druker. They suggest that  $\mu^3$ -coordination produces a more stable sulfur-containing end-product (a  $\mu^3$ -coordinated sulfide vs an  $\text{HS}^\bullet$  radical) and allows the oxidation, which must occur when the organic product is eliminated, to be spread out over the entire metal framework rather than localized on the sulfur atom. This lowers the bond dissociation energy and activates the S–C bond. Bimetallic thiophene-bridged complexes may favor formation of these trimetallic intermediates.

### Computational Details

The molecular structures of the metal-inserted complex **6** and the bridged adduct **7** have been determined by X-ray diffraction.<sup>16</sup> These known structures were used for the non-empirical, approximate Hartree–Fock, Fenske–Hall molecular orbital calculations.<sup>54</sup> The 1s through *nd* functions for Ni were generated by a best fit to Herman–Skillman<sup>55</sup> atomic calculations using the method of Bursten, Jensen, and Fenske.<sup>56</sup> The (*n*+1)s and (*n*+1)p functions were chosen to have exponents of 2.0 for Ni. The carbon and sulfur functions were taken from the double- $\zeta$  functions of Clementi.<sup>57</sup> The valence p functions were retained as the double- $\zeta$  functions, while all the other functions were reduced to single- $\zeta$  functions. An exponent of 1.2 was used for hydrogen. Orbital populations, bond overlap populations, and atomic charges were determined with Mulliken population analyses.<sup>58,59</sup> Bond orders were calculated using the method described by Sannigrahi.<sup>60</sup>

(54) Hall, M. B.; Fenske, R. F. *Inorg. Chem.* **1972**, *11*, 768–775.

(55) Herman, F.; Skillman, S. *Atomic Structure Calculations*; Prentice Hall: Englewood Cliffs, NJ, 1963.

(56) Bursten, B. E.; Jensen, J. R.; Fenske, R. F. *J. Chem. Phys.* **1978**, *68*, 3320–3321.

(57) Clementi, E. *J. Chem. Phys.* **1964**, *40*, 1944–1945.

Molecular mechanics calculations on the dinickel DBT-bridged complex **8** were performed using the 1.02 Universal Force Field<sup>61–63</sup> as implemented through Cerius<sup>2</sup>.<sup>64</sup> The atoms were typed in accordance with the force field.

The transition state between the two conformers of  $[(\text{CO}_3)\text{-Fe}]_2(\eta\text{-T})$  was calculated using the Gaussian-98 package.<sup>65</sup> The level of theory was DFT/B3LYP. For the Fe atom, the relativistic effective core potential (RECP) of Hay and Wadt,<sup>66</sup> which treats the outermost core orbitals ( $5s^25p^6$ ) as valence, was employed (LanL2DZ). For all other atoms, the 6-311G\*\* basis set was used.

**Acknowledgment.** Financial support of this research by the National Science Foundation (Grants CHE-9421784 and CHE-9817857) is greatly appreciated. We also thank Dr. W. D. Jones for continually providing us with valuable insights and unpublished results.

OM991005B

(58) Mulliken, R. S. *J. Chem. Phys.* **1955**, *23*, 1833–1840.

(59) Mulliken, R. S. *J. Chem. Phys.* **1955**, *23*, 1841–1846.

(60) Sannigrahi, A. B.; Kar, T. *J. Chem. Educ.* **1988**, *65*, 674–676.

(61) Casewit, C. J.; Rappé, A. K.; Colwell, K. S. *J. Am. Chem. Soc.* **1992**, *114*, 10035–10045.

(62) Casewit, C. J.; Rappé, A. K.; Colwell, K. S.; Goddard, W. A., III; Skiff, W. M. *J. Am. Chem. Soc.* **1992**, *114*, 10024–10035.

(63) Casewit, C. J.; Rappé, A. K.; Colwell, K. S. *J. Am. Chem. Soc.* **1992**, *114*, 10046–10053.

(64) *Cerius<sup>2</sup>*; 3.8; Molecular Simulations Incorporated: San Diego, CA, 1998.

(65) Frisch, M. J.; Trucks, G. W.; Schlegel, H. B.; Scuseria, G. E.; Robb, M. A.; Cheeseman, J. R.; Zakrzewski, V. G.; Montgomery, J. A.; Stratman, R. E.; Burant, J. C.; Dapprich, S.; Millam, J. M.; Daniels, A. D.; Kudin, K. N.; Strain, M. C.; Farkas, O.; Tomasi, J.; Barone, V.; Cossi, M.; Cammi, R.; Mennucci, B.; Pomelli, C.; Adamo, C.; Clifford, S.; Ochterski, J.; Petersson, G. A.; Ayala, P. Y.; Cui, Q.; Morokuma, K.; Malick, D. K.; Rabuck, A. D.; Raghavachari, K.; Foresman, J. B.; Cioslowski, J.; Ortiz, J. V.; Stefanov, B. B.; Liu, G.; Liashenko, A.; Piskorz, P.; Komaromi, I.; Gomperts, R.; Martin, R. L.; Fox, D. J.; Keith, T.; Al-Laham, M. A.; Peng, C. Y.; Nanayakkara, A.; Gonzales, C.; Challacombe, M.; Gill, P. M. W.; Johnson, B.; Chen, W.; Wong, M. W.; Andres, J. L.; Gonzales, C.; Head-Gordon, M.; Replogle, E. S.; Pople, J. A. *Gaussian*, Revision A.5; Gaussian, Inc.: Pittsburgh, PA, 1998.

(66) Hay, P. J.; Wadt, W. R. *J. Chem. Phys.* **1985**, *82*, 299–310.